Flexibility in Multi-Energy Communities With Electrical and Thermal Storage: A Stochastic, Robust Approach for Multi-Service Demand Response

Nicholas Good, *Member, IEEE*, and Pierluigi Mancarella, *Senior Member, IEEE*

***Abstract*—There is increasing interest in multi-energy communities, which could become important sources of demand response flexibility, especially when equipped with storage. Their location on distribution networks mean their exploitation to solve local capacity congestions may be particularly valuable, whilst their ability to partake in energy/reserve markets can improve their business cases. However, maximizing this flexibility potential by providing multiple services that are subject to uncertain calls is a challenging modeling task. To address this, we present a stochastic energy/reserve mixed integer linear program for a community energy system with consideration of local network constraints. By covering all the relevant energy vectors, the multi-energy formulation allows comprehensive modeling of different flexibility options, namely, multi-energy storage, energy vector substitution, end-service curtailment, and power factor manipulation. A key feature of the approach is its robustness against any reserve call, ensuring that occupant thermal comfort cannot be degraded beyond agreed limits in the event of a call. The approach is demonstrated through a case study that illustrates how the different flexibility options can be used to integrate more electric heat pumps into a capacity constrained smart district that is managed as a community energy system, while maximizing its revenues from multiple markets/services.**

***Index Terms*—Multi-energy systems, community energy systems, smart district, flexibility, energy storage, batteries, demand response.**

Nomenclature

Acronyms

BES	Battery energy store
CHP	Combined heat and power
COP	Coefficient of performance
DHW	Domestic hot water
DNO	Distribution network operator
DR	Demand response
EB	Electric boiler
EHP	Electric heat pump
ESCo	Energy services company
ETD	Expected thermal discomfort
GB	Gas boiler
MILP	Mixed integer linear program
SH	Space heating
SOC	State of charge
TES	Thermal energy store.

Indices

s	index of scenarios, 1 to N_s
i	index of settlement periods, 1 to N_i
l	index of locations, 1 to N_l
b	discrete number, 1 to N_b
α	index of flexible devices $\{EHP, EB, CHP, solar, wind, BES\}$.

Parameters

Resource:

B_l^{min}/B_l^{max}	battery min/max capacity (kWh)
C_l^b/Cx_l	building/TES thermal capacitance (kWh/°C)
$E_{s,i,l}^{load}$	non-heating (base) electricity load (kWh)
H_l^{CHPmin}	CHP min heating power (kW)
H_l^{CHPmax}	CHP max heating power (kW)
$H_{s,i,l}^{DHW}$	DHW heating load (kWh)
H_l^{EBmin}	EB min heating power (kW)
H_l^{EBmax}	EB max heating power (kW)
H_l^{GBmin}	GB min heating power (kW)
H_l^{GBmax}	GB max heating power (kW)
$Int_{s,i,l}$	internal (metabolic) heat gains (kW)
$O_{s,i,l}$	binary occupancy/heat required indicator (-)
P_l^{BESmin}	battery min charge rate (kW)
P_l^{BESmax}	battery max charge rate (kW)
P_l^{EHPmin}	EHP min electrical power (kW)
P_l^{EHPmax}	EHP max electrical power (kW)
$P_{s,i,l}^{solar}$	solar electrical power (kW)
$P_{s,i,l}^{wind}$	wind electrical power (kW)

Manuscript received February 16, 2017; revised June 28, 2017; accepted August 12, 2017. Date of publication September 28, 2017; date of current version December 19, 2018. This work was supported in part by EC FP7 DIMMER Project under Grant 609084, and in part by U.K. EPSRC MY-STORE Project under Grant EP/N001974/1. Paper no. TSG-00229-2017. *(Corresponding author: Nicholas Good.)*

N. Good is with the School of Electrical and Electronic Engineering, University of Manchester, Manchester M13 9PL, U.K. (e-mail: nicholas.good@manchester.ac.uk).

P. Mancarella is with the Department of Electrical and Electronic Engineering, University of Melbourne, Melbourne, VIC 3010, Australia, and also with the University of Manchester, Manchester M13 9PL, U.K. (e-mail: pierluigi.mancarella@unimelb.edu.au).

Color versions of one or more of the figures in this paper are available online at http://ieeexplore.ieee.org.

Digital Object Identifier 10.1109/TSG.2017.2745559

R_l^b/Rx_l	building/TES thermal resistance (°C/kW)
$R_{i,l}^{resd}/R(d)^{resd}$	max device/district apparent power (kW)
$Sol_{s,i,l}$	solar heat gains (kW)
$T_{i,l}^{set}$	set temperature (°C)
X_l^{min}/X_l^{max}	min/max temperature of TES (°C)
$\delta_{i,l}^{low}/\delta_{i,l}^{high}$	max down/up variation from set temp (°C)
η_l^e/η_l^t	CHP unit electrical/thermal efficiency (-)
η_l^{GB}/η_l^{EB}	gas/electric boiler efficiency (-)
φ_l	battery round-trip efficiency (-)
$\gamma_{s,i,l}^{EHP}$	EHP coefficient of performance (-).

Price/Weather Profiles and Parameters:

c^{maxd}	max call length for down/up reserve (hours)
P^{dcall}	probability of up/down reserve call (-)
p_s	scenario probability (-)
$T_{s,i}^{out}$	outside temperature (°C)
λ_i/ρ_i	day-ahead electricity/gas price (£/kWh)
$\mu_{s,i}^-/\mu_{s,i}^+$	imbalance import/export price (£/kWh)
π_i^d	down reserve availability price (£/kW)
ω_i^d	down reserve window (-)
$\varsigma_i^-/\varsigma_i^+$	temperature deficit/surplus penalties (£/°Ch)
χ	reactive power supply penalty (£/kVar).

Time-Band Length:

t	length of time step (h).

Variables

$B_{s,i,l}$	battery energy level (%)
$Bres_{s,i,l}^d$	building thermal storage footroom (kW)
D_i^-/D_i^+	day-ahead energy import/export (kW)
$G_{s,i,l}^{GB}$	GB gas power (kW)
$G(d)_{s,i}^-$	gas import, district level (kW)
$H_{s,i,l}^{in}/H_{s,i,l}^{out}$	heat in/out to TES (kWh)
$H_{s,i,l}^{SH}$	space heating demand (kWh)
$I_{s,i}^-/I_{s,i}^+$	imbalance energy import/export (kW)
$P_{s,i,l}^{BES+}/P_{s,i,l}^{BES-}$	battery export/import power (kW)
$P_{s,i,l}^{CHP}/P_{s,i,l}^{EHP}$	CHP/EHP electrical power (kW)
$P_{s,i,l}^{EB}$	EB electrical power (kW)
$P_{s,i,l}^{\alpha}/P(d)_{s,i}$	device/district active power (kW)
$Q_{s,i,l}^{\alpha}/Q(d)_{s,i}$	device/district reactive power (kW)
$R_{s,i,l}^{BESd}/R_{s,i,l}^{CHPd}$	down reserve (battery/CHP) (kW)
$R_{s,i,l}^{EBd}/R_{s,i,l}^{EHPd}$	down reserve (EB/EHP) (kW)
$S_{s,i,l}^{\alpha}/S(d)_{s,i}$	device/district apparent power (kW)
$T_{s,i,l}$	indoor temperature (°C)
$T_{s,i,l}^+/T_{s,i,l}^-$	temperature surplus/deficit (°C)
$Tr_{s,i,l}^-/Tr_{s,i,l}^+$	temperature surplus/deficit |reserve call (°C)
$X_{s,i,l}$	energy level of thermal energy store (kWh)
$X_{s,i,l}^{loss}$	TES heat loss (kWh)
$z_{s,i,l}$	binary battery import/export indicator (-)
$\alpha_{s,i,l}$	internal/solar gain vent variable (%).

I. INTRODUCTION

DEMAND for flexibility in electricity systems is expected to grow as penetration of electric heating, electric transport, and variable and/or inflexible generation grows [1]. In particular, demand response (DR), including from storage, has been identified as an attractive source of such flexibility. This is due to the limited additional investment (and the opportunity to disperse the investment amongst building owners) and advances in information and communication technology, in particular with regard to small-scale energy management systems [1], [2].

DR resources do, however, present difficulties. One issue is the propensity of technologies to cluster geographically, for social reasons [3]. This is pertinent given the limited capacity of local electricity distribution networks (which are expensive to expand) and which may become strained as adoption of electric heating/transport increases, increasing peak loads [4]. Further, DR can result in synchronization of loads (or local generation), reducing the natural diversity of demand and threatening local network capacity limits [5]. Hence suitable local management of DR aggregation is needed.

Community energy systems [6], or smart districts [7], are an ideal setup to prevent local issues and at the same time maximize the DR potential from local resources, and are attracting increasing interest. In particular, many modelling approaches are now explicitly recognizing the importance of modelling *energy*, rather than simply *electricity*, generation, storage and consumption, for both operation and investment [8]–[11], in a multi-energy system context [12]. DR resources in general, and community energy systems in particular, typically incorporate multiple energy vectors, and hence can be regarded as small-scale multi-energy systems that can exploit their intrinsic multi-energy flexibility.

For any DR resource a natural objective is maximization of revenues from DR (whilst managing local network constraints). To do this DR resources must provide multiple services to multiple actors, requiring participation in all available markets [13]–[15]. As an increasing number of devices (e.g., battery storage, photovoltaic systems, etc.), are equipped with power electronic interfaces, provision of multiple services should consider optimization of both active and reactive power [13]. A complicating factor in optimizing provision of these multiple services is the substantial uncertainty (in demand, service calls and prices) faced by DR resources [8]. Thus optimization approaches employed by DR resources should be stochastic. Given that DR resources often have the potential to effect consumer comfort (e.g., their thermal comfort) approaches should ensure results are robust against any reserve call, with respect to thermal comfort [16].

Many published works address some of these aspects. In particular there is a large amount of work on DR considering the electricity vector and focused on storage. Within this set several works consider the key aspects of considering multiple markets/services under uncertainty [13], [14], [17]–[22]. Within these references all consider energy and some sort of reserve market (except [21], which consider energy and a demand charge) and all appreciate the necessity of reserving enough energy within the battery to provide any committed reserve if called. Additionally [13], [14], [17], [18] consider the effect of distribution network (transformer or line) constraints, although only [13] considers the effect of reactive power (albeit through an outer-linearization of the network capacity constraint which may allow some violation of the true non-linear network capacity constraint). For illustration of the value of multiple services [20] is particularly useful: a key finding is that many services may be synergic (see also [23] for more discussion), allowing revenues to be 'stacked', and that this may be necessary to cover battery investment costs. Considering DR from multi-energy systems there is significant work considering provision of DR. In [24] DR from substitution of energy vectors/technologies is considered whilst [8], [25]–[27] consider how combined heat and power (CHP) and/or electric heat pumps (EHP), can use heat storage from a thermal energy store (TES) and/or building fabric to perform energy arbitrage. Further, there is some work considering provision of multiple services from CHP-based systems. References [28]–[30] all consider the joint provision of energy arbitrage and reserve, although these works either do not consider excess or deficit heat in the event of a reserve call. Considering the wider class of thermostatic loads [31], [32] present a model which is designed to exploit large groups of thermostatic appliances to provide energy arbitrage and reserve. These works include constraints to ensure that any solution is robust against any reserve call, i.e., that appliances will not violate their operating limits if reserve is called. However, it is acknowledged that, to make the formulation applicable for large groups of appliances (a requirement that is not necessary for community-level optimization) the result is conservative. From the analyzed literature on multi-energy systems it is therefore notable how there is relatively little consideration of uncertainty, overall.

As demonstrated there has been significant work which addresses the provision of multiple services, from multiple types of community-level, multi-energy flexibility. However there exist several gaps in the existing literature, which require attention. Firstly, the most developed work on multi-service provision from demand-side resources focuses on electrical storage, with many works considering a wide range of services and featuring sophisticated treatments of uncertainty. The work on community-level multi-energy systems is less developed in these aspects. Hence, there exists a gap for an approach which systematically incorporates flexibility from *multi-energy storage, substitution* (of energy vectors/devices), *curtailment* (of energy services) and *power factor manipulation*, considering a distribution network operator service, for relief of network congestion, as well as energy arbitrage and reserve. Secondly, although [13], [32] recognizes the necessity of ensuring any reserve commitment is robust against a reserve call (in a deterministic formulation), a general, stochastic problem formulation, which ensures reserve commitment from any type of the above flexibilities is robust with respect to thermal comfort, is missing.

In response to these gaps, this work presents a stochastic, smart district optimization model for DR resources in a community energy system/district. In the formulation, as in [8], all buildings in the district contract with a retailer-energy services company (ESCo), who controls the flexible devices, procures/sells energy, and provides thermal comfort to building occupants. In particular the model enables optimization of multi-energy storage, substitution and curtailment DR, with consideration of device/district active and reactive power, to provide multiple services, ensuring any result is robust against any call for any reserve service, in any modelled scenario. Given the significant flexibility inherent in building fabric and heating systems [8], [33], this model focuses on flexibility from building thermal systems and associated electro-thermal technologies as well as batteries, although it may be extended to include other sources of flexibility (e.g., electric vehicles).

In the remainder of this paper, a description of the problem formulation is given in Section II. Afterwards, in Section III, the model is demonstrated through application to a case study considering a techno-economic assessment of electric heat pump integration in a community (district) of fifty detached houses on a constrained feeder, enabled by various types of flexibility. Concluding remarks are given in Section IV.

II. Problem Description

The district resources are modelled using a mixed integer linear programming (MILP) model. Utilization of a MILP formulation is necessary to disallow simultaneous battery charging and discharging. Below, formulation of plant, storage and building models, the reserve allocation model, and active/reactive power constraints are detailed. Subsequently, the formulation of district level balances and district active/reactive power constraints are detailed, before the district objective function is presented.

A. Modelling the Resource

1) Heating Plant and Storage Operating Limits: Constraints (1)-(4) detail the limits of four common electrical/gas heat generators: gas boiler (GB), CHP, EHP and electric boiler (EB).

$$H_l^{GBmin} \le G_{s,i,l}^{GB}\eta_l^{GB} \le H_l^{GBmax} \quad (1)$$

$$H_l^{CHPmin} \le \frac{P_{s,i,l}^{CHP}\eta_l^t}{\eta_l^e} \le H_l^{CHPmax} \quad (2)$$

$$P_l^{EHPmin} \le P_{s,i,l}^{EHP} \le P_l^{EHPmax} \quad (3)$$

$$H_l^{EBmin} \le P_{s,i,l}^{EB}\eta_{s,i,l}^{EB} \le H_l^{EBmax} \quad (4)$$

For all $s = 1$ to N_s, $ix = 0$ to N_i, $l = 1$ to N_l.

As detailed by (5) and (6), district building temperatures must remain within a band around the target temperature ($T_{i,l}^{set}$), determined by building thermal storage parameters ($\delta_{i,l}^{high}$ and $\delta_{i,l}^{low}$), whenever the building is actively occupied and the outdoor temperature is above a set threshold (indicated by $O_{s,i,l}$) [8]. $T_{s,i,l}^{+}$ and $T_{s,i,l}^{-}$ enable buildings to deviate from the allowed temperature bounds. These variables can be used to enable trading of thermal comfort [8], or can be set punitively high, so that such deviation only occurs to when the dynamics of the building make it impossible to satisfy thermal comfort constraints without their use.

The district may include both TES and battery energy store (BES). TES operating limits are set according to (7). Constraints (8)-(10) set the limits on battery energy level, charge and discharge power. The binary variables ensure that the battery does not charge and discharge at the same time.

$$O_{s,i,l}\left(T_{s,i,l} - T_{s,i,l}^{+}\right) \le O_{s,i,l}\left(T_{i,l}^{set} + \delta_{i,l}^{high}\right) \quad (5)$$

$$O_{s,i,l}\left(T^{set}_{i,l} - \delta^{low}_{i,l}\right) \leq O_{s,i,l}\left(T_{s,i,l} + T^{-}_{s,i,l}\right) \tag{6}$$

$$\left(X^{min}_{l} - T_{s,i,l}\right)Cx_l \leq X_{s,i,l} \leq \left(X^{max}_{l} - T_{s,i,l}\right)Cx_l \tag{7}$$

$$B^{min}_{l} \leq B_{s,i,l} \leq B^{max}_{l} \tag{8}$$

$$z_{s,i,l}P^{BESmin}_{l} \leq P^{BES+}_{s,i,l} \leq z_{s,i,l}P^{BESmax}_{l} \tag{9}$$

$$\left(1 - z_{s,i,l}\right)P^{BESmin}_{l} \leq P^{BES-}_{s,i,l} \leq \left(1 - z_{s,i,l}\right)P^{BESmax}_{l} \tag{10}$$

For all $s = 1$ to N_s, $i = 0$ to N_i, $l = 1$ to N_l.

2) Initialization: To ensure that the produced results are not distorted, the value of any energy stored within TES or battery, at the initial time-step must be set as equal to the last time-step, (11) and (12).

$$X_{s,0,l} = X_{s,N_i,l} \tag{11}$$

$$B_{s,0,l} = B_{s,N_i,l} \tag{12}$$

For all $s = 1$ to N_s, $l = 1$ to N_l.

3) Building and Storage System Equations: Equation (13) defines the building temperature. This is determined by temperature in the previous time-step, heat loss to the environment, heat gain from the TES ($X^{loss}_{s,i,l}$, defined in (14)), space heating heat from the TES ($H^{SH}_{s,i,l}$), and internal and solar heat gain ($Int_{s,i,l}$ and $Sol_{s,i,l}$). This heat gain may be reduced through occupant actions (e.g., opening windows) to reduce the building temperature. This effect is modelled by $\alpha_{s,i,l}$, the percentage of heat vented.

For each TES, the heat from various generator types is aggregated into a TES heat input variable (15). This heat input, along with the heat loss to the building, the delivered space heating (SH) and domestic hot water (DHW), and the state of the TES at the current time-step, determines the TES state at the next time-step (16). For the battery, the energy level in the next time step is determined by the current energy level and the charging and discharging power, the latter adjusted to factor in the battery round-trip efficiency (17).

$$\begin{aligned} T_{s,i+1,l} = T_{s,i,l} + \Big(H^{SH}_{s,i,l} + \left(1 - \alpha_{s,i,l}\right)\left(Int_{s,i,l} + Sol_{s,i,l}\right) \\ - \left(T_{s,i,l} - T^{out}_{s,i}\right)tR^{b^{-1}}_{l}\Big)C^{b^{-1}}_{l} + X^{loss}_{s,i,l} \end{aligned} \tag{13}$$

$$X^{loss}_{s,i,l} = \frac{\left(\frac{X_{s,i,l}}{Cx_l} - T_{s,i,l}\right)t}{Rx_l} \tag{14}$$

$$G^{GB}_{s,i,l}\eta^{GB}_{l} + \frac{P^{CHP}_{s,i,l}\eta^{t}_{l}t}{\eta^{e}_{l}} + P^{EHP}_{s,i,l}\gamma^{EHP}_{s,i,l}\mathrm{t} + P^{EB}_{s,i,l}\eta^{EB}_{l}\mathrm{t} = H^{in}_{s,i,l} \tag{15}$$

$$X_{s,i+1,l} = X_{s,i,l} + H^{in}_{s,i,l} - X^{loss}_{s,i,l} - H^{SH}_{s,i,l} - H^{DHW}_{s,i,l} \tag{16}$$

$$B_{s,i+1,l} = B_{s,i,l} + \left(P^{BES-}_{s,i,l} - P^{BES+}_{s,i,l}/\varphi_l\right)t \tag{17}$$

$$H^{SH}_{s,i,l} \geq 0 \tag{18}$$

For all $s = 1$ to N_s, $i = 0$ to N_i, $l = 1$ to N_l.

B. Reserve Modelling

A critical part of the problem formulation is the constraint set which define the volume of reserve. Due to space restrictions only the formulation for down (consumption) reserve is presented. Extension to up consumption reserve is straightforward. A formulation which includes such reserve (though without constraints to ensure robustness with respect to thermal comfort) is presented in [34].

Constraints (19)-(23) limit reserve by the reserve available from the flexible devices. As shown in constraints (20)-(22), EHP and EB down-reserve can be no greater than the footroom in these devices, whilst CHP down-reserve can be no greater than the device headroom. For a BES, down-reserve can be no greater than the maximum discharge rate (23).

$$R^{resd}_{i,l} = R^{EHPd}_{s,i,l} + R^{EBd}_{s,i,l} + R^{CHPd}_{s,i,l} + R^{BESd}_{s,i,l} \tag{19}$$

$$0 \leq R^{EHPd}_{s,i,l} \leq P^{EHP}_{s,i,l} - P^{EHPmin}_{l} \tag{20}$$

$$0 \leq R^{EBd}_{s,i,l} \leq P^{EB}_{s,i,l} - \frac{H^{EBmin}_{l}}{\eta^{EB}_{l}} \tag{21}$$

$$0 \leq R^{CHPd}_{s,i,l} \leq \frac{H^{CHPmax}_{l}\eta^{e}_{l}}{\eta^{t}_{l}} - P^{CHP}_{s,i,l} \tag{22}$$

$$0 \leq R^{BESd}_{s,i,l} \leq P^{BESmax}_{l} + P^{BES-}_{s,i,l} - P^{BES+}_{s,i,l} \tag{23}$$

For all $s = 1$ to N_s, $i = 0$ to N_i, l= 1 to N_l.

To ensure that the formulation is robust with respect to occupant thermal comfort (i.e., that any reserve call does not result in violations of thermal comfort standards) it is necessary to ensure that there is enough thermal energy in storage (TES or building fabric), or that there is an adequate alternative source of heat on stand-by to ensure that thermal comfort can be met at all times. Constraints (24)-(28) do this through a novel approach which constrains the committed reserve, by device, by the amount of stored thermal energy. Constraint (24) limits down-consumption reserve from electro-thermal devices by sum of the TES footroom (divided by the maximum reserve call length), the building fabric footroom ($Bres^{d}_{s,i,l}$) and the gas boiler headroom. As robustness against thermal comfort degradation is only required when the building is actively occupied and heating is required (i.e., $O_{s,i,l} = 1$), constraint (24) is only valid when this condition holds.

Constraint (26) sets the building fabric footroom, defined by the building temperature ($T_{s,i,l}$), the set temperature ($T^{set}_{i,l}$) and the building flexibility parameter ($\delta^{low}_{i,l}$). Variable $Tr^{-}_{s,i,l}$ allows comfort to be traded in the event of a reserve call.

Constraint (28) similarly ensures there is enough footroom in the battery so that the solution is robust to any reserve call.

$$\begin{aligned} &O_{s,i,l}\left(R^{EHPd}_{s,i,l}\gamma^{EHP}_{s,i,l} + R^{EBd}_{s,i,l}\eta^{EB}_{l} - R^{CHPd}_{s,i,l}\eta^{t}_{l}/\eta^{e}_{l}\right) \\ &\quad \leq O_{s,i,l}\left(\frac{\left(\frac{X_{s,i,l}}{Cx_l} + T_{s,i,l} - X^{min}_{l}\right)Cx_l + Bres^{d}_{s,i,l}}{call^{maxd}t} + \left(H^{GBmax}_{l} - \frac{H^{GB}_{s,i,1}}{t}\right)\right) \end{aligned} \tag{24}$$

$$\begin{aligned} &O_{s,i,l}R^{CHPd}_{s,i,l}\eta^{t}_{l}/\eta^{e}_{l} \\ &\quad \leq O_{s,i,l}\left(\frac{\left(X^{max}_{l} - \frac{X_{s,i,l}}{Cx_l} + T_{s,i,l}\right)Cx_l + Bres^{u}_{s,i,l}}{call^{maxd}t} + \frac{H^{GB}_{s,i,1}}{t}\right) \end{aligned} \tag{25}$$

$$0 \leq Bres^{d}_{s,i,l} = \frac{O_{s,i,l}\left(T_{s,i,l} - \left(T^{set}_{i,l} - \delta^{low}_{i,l}\right) + Tr^{-}_{s,i,l}\right)C^{b}_{l}}{t} \tag{26}$$

$$0 \le Bres^{u}_{s,i,l} = \frac{O_{s,i,l}\left(\left(T^{set}_{i,l} + \delta^{high}_{i,l}\right) - T_{s,i,l} + Tr^{+}_{s,i,l}\right)C^{b}_{l}}{t} \tag{27}$$

$$R^{BESd}_{s,i,l} \le B_{s,i,l}/\left(call^{maxd}t\right) \tag{28}$$

For all s = 1 to N_s, i = 0 to N_i, l= 1 to N_l.

C. Device Active and Reactive Power Constraints

To enable modelling of active and reactive power within a MILP model this work uses a linear approximation (30) of device real power constraint (29), for any potentially flexible device. As opposed to the method detailed in [13], this discretization results in the feasible area defined by the linear constraints lying entirely within the feasible area defined by the non-linear constraint (29). This is important as when the real power constraints are active for extended periods. In (29) and (30) A is the set of flexible devices $\{EHP, EB, CHP, solar, wind, BES\}$, and N_b is half of the number of linear constraints in approximation of (29), as defined by the user.

$$\left(P^{\alpha}_{s,i,l}\right)^2 + \left(Q^{\alpha}_{s,i,l}\right)^2 \le \left(S^{\alpha}_{s,i,l}\right)^2 \tag{29}$$

$$\begin{aligned}&\left(Q^{\alpha}_{s,i,l} - S^{\alpha}_{s,i,l}\cos\left(\frac{(b-1)\pi}{N_b}\right)\right)\left(\frac{\sin\left(\frac{b\pi}{N_b}\right) - \sin\left(\frac{(b-1)\pi}{N_b}\right)}{\cos\left(\frac{b\pi}{N_b}\right) - \cos\left(\frac{(b-1)\pi}{N_b}\right)}\right)\\&+ S^{\alpha}_{s,i,l}\sin\left(\frac{(b-1)\pi}{N_b}\right) \le P^{\alpha}_{s,i,l}\\&\le \left(Q^{\alpha}_{s,i,l} + S^{\alpha}_{s,i,l}\cos\left(\frac{(b-1)\pi}{N_b}\right)\right)\left(\frac{\sin\left(\frac{b\pi}{N_b}\right) - \sin\left(\frac{(b-1)\pi}{N_b}\right)}{\cos\left(\frac{b\pi}{N_b}\right) - \cos\left(\frac{(b-1)\pi}{N_b}\right)}\right)\\&- S^{\alpha}_{s,i,l}\sin\left(\frac{(b-1)\pi}{N_b}\right)\end{aligned} \tag{30}$$

For all $s = 1$ to N_s, $i = 0$ to N_i, $l = 1$ to N_l, $b = 1$ to N_b, $\alpha \in A$.

D. Energy/Power/Reserve Balances

For optimization at the district level (31), (32) and (34) sum up district electricity and gas consumption, and reserve provision to the district level. As shown, electricity is procured through a combination of available markets (day-ahead and imbalance markets, in this formulation). The distinction between import and export electricity prices are necessary as import and export prices may not be equivalent.

$$\begin{aligned}\mathrm{D}^{-}_{i} - \mathrm{D}^{+}_{i} + I^{-}_{s,i} - I^{+}_{s,i} = &\frac{E^{load}_{s,i,l}}{t} + P^{EHP}_{s,i,l} + P^{EB}_{s,i,l} - P^{CHP}_{s,i,l}\\&- P^{solar}_{s,i,l} - P^{wind}_{s,i,l} + P^{BES-}_{s,i,l} - P^{BES+}_{s,i,l}\end{aligned} \tag{31}$$

$$G(d)^{-}_{s,i} = \frac{P^{CHP}_{s,i,l}\eta^{t}_{l}t}{\eta^{e}_{l}} + G^{GB}_{s,i,l} \tag{32}$$

$$\mathrm{D}^{-}_{i}, \mathrm{D}^{+}_{i}, I^{-}_{s,i}, I^{+}_{s,i}, G(d)^{-}_{s,i} \ge 0 \tag{33}$$

For all s = 1 to N_s, i = 0 to N_i.

Following common practice [14], committed reserve must be the same, across all windows. Equation (34) ensures this, whilst allowing for the reserve contributed by each location to vary by scenario, and time-step. This approach can offer significant benefits, in terms of reserve commitment, for resources which are uncertain, yet diverse.

$$\omega^{d}_{i}R(d)^{resd} = \omega^{d}_{i}\sum\nolimits_{l=1}^{N_l} R^{resd}_{s,i,l} \tag{34}$$

For all s = 1 to N_s, i = 0 to N_i.

In order to ensure that district real power constraints (e.g., deriving from network capacities) are respected, load and device reactive powers are summed to the district level (35).

$$Q(d)_{s,i} = \sum_{l=1}^{N_l}\left(\frac{\gamma E^{load}_{s,i,l}}{t} + \sum\nolimits_{\alpha \in A} Q^{\alpha}_{s,i,l}\right) \tag{35}$$

For all s = 1 to N_s, i = 0 to N_i.

E. District Active and Reactive Power Constraints

Following the same approach as in (30), (36) defines the linear approximation of the district real power constraint.

$$\begin{aligned}&\left(Q(d)_{s,i} - S(d)_{s,i}\cos\left(\frac{(b-1)\pi}{N_b}\right)\right)\\&\times\left(\frac{\sin\left(\frac{b\pi}{N_b}\right) - \sin\left(\frac{(b-1)\pi}{N_b}\right)}{\cos\left(\frac{b\pi}{N_b}\right) - \cos\left(\frac{(b-1)\pi}{N_b}\right)}\right) + S(d)_{s,i}\sin\left(\frac{(b-1)\pi}{N_b}\right)\\&\le P(d)_{s,i} \le \left(Q(d)_{s,i} + S(d)_{s,i}\cos\left(\frac{(b-1)\pi}{N_b}\right)\right)\\&\times\left(\frac{\sin\left(\frac{b\pi}{N_b}\right) - \sin\left(\frac{(b-1)\pi}{N_b}\right)}{\cos\left(\frac{b\pi}{N_b}\right) - \cos\left(\frac{(b-1)\pi}{N_b}\right)}\right) - S(d)_{s,i}\sin\left(\frac{(b-1)\pi}{N_b}\right)\end{aligned} \tag{36}$$

For all s = 1 to N_s, i = 0 to N_i, l= 1 to N_l, b = 1 to N_b.

F. Objective

The district objective function is given in (37). As shown, the retailer-ESCo buys and sells electricity at import/export prices in the day-ahead market (λ^{-}_{i}, λ^{+}_{i}) and in the imbalance market ($\mu^{-}_{s,i}$, $\mu^{+}_{s,i}$), whilst gas is purchased at the gas import price (ρ_i). District down reserve is remunerated according to the appropriate availability prices (π^{d}_{i}). Temperature deficit and surplus are penalized according to the appropriate penalties (ς^{+}_{i}, ς^{-}_{i}), which may be considered a payment from the retailer-ESCo to building occupants. Similarly, $Tr^{-}_{s,i,l}$ is penalized according to ς^{-}_{i}, adjusted by the probability of a reserve call P^{dcall}. Finally, reactive power supply is penalized by a small value χ. This represents the cost of inverter operation, which although small, is useful as it prevents the reactive power supply from varying when network constraints are not binding.

$$\begin{aligned}Min\Bigg\{\sum_{s=1}^{N_s}\Bigg[p_s\sum_{i=1}^{N_i}\Bigg(&\lambda^{-}_{i}\mathrm{D}^{-}_{i}\mathrm{t} - \lambda^{+}_{i}\mathrm{D}^{+}_{i}\mathrm{t} + \mu^{-}_{s,i}I^{-}_{s,i}\mathrm{t}\\&- \mu^{+}_{s,i}I^{+}_{s,i}\mathrm{t} + \rho_i G(d)^{-}_{s,i}\mathrm{t} - \pi^{d}_{i}R(d)^{resd}t\\&+ \sum_{l=1}^{N_l}\Bigg(\varsigma^{+}_{i}T^{+}_{s,i,l} + \varsigma^{-}_{i}T^{-}_{s,i,l} + P^{dcall}\varsigma^{-}_{i}Tr^{-}_{s,i,l}\\&+ \chi\sum_{\alpha \in A} Q^{\alpha}_{s,i,l}\Bigg)\Bigg)\Bigg]\Bigg\}.\end{aligned} \tag{37}$$

TABLE I
DESCRIPTION OF TESTS ACCORDING TO EHP INTEGRATION, MARKETS CONSIDERED AND TYPE OF FLEXIBILITY AVAILABLE

No	Full EHP integration?	Markets	Flexibility
0	No	Energy	None
1	Yes	Energy	Thermal storage
2	Yes	Energy	Auxiliary gas boiler
3	Yes	Energy	Battery
4	Yes	Energy	Battery with power factor control
5	Yes	Energy	Building temperature flexibility (up)
6	Yes	Energy	Building temperature flexibility (up/down)
7	Yes	Energy+Reserve	Thermal storage
8	Yes	Energy+Reserve	Auxiliary gas boiler
9	Yes	Energy+Reserve	Battery
10	Yes	Energy+Reserve	Battery with power factor control
11	Yes	Energy+Reserve	Building temperature flexibility (up)
12	Yes	Energy+Reserve	Building temperature flexibility (up/down)

III. CASE STUDY APPLICATIONS

To demonstrate application of the model a case study which compares several tests is presented. In the first set of tests the ability of the model to assess how various types of district flexibility can be employed to enable the integration of new low-carbon electricity loads is demonstrated, following an energy cost minimization objective. In this case, integration of EHP is considered. As shown in Table I, tests 1-6 utilize different types of flexibility to avoid network constraints, to enable full integration of EHP. In each test the minimum size resource to enable full integration is identified. These tests can be compared, using various metrics, against the base case (0). In test 1 TES are placed in each building, to enable shifting of EHP operation, whilst in test 2 a gas boiler is used to avoid EHP operation at peak times. In tests 3 and 4 a BES is used to reduce grid import of active power, and, for test 4, to additionally manipulate the BES inverter power factor to absorb district reactive power, to reduce real power loads. Tests 5 and 6 introduce bands above (test 5) or above and below (test 6) the target temperature, in which the building temperature may vary during times of active occupancy. In the second set of tests (7-13), provision of reserve is also considered, to demonstrate the potential of different types of district flexibility to provide reserve. Subsequently, cash flows for different combinations of services are presented to identify synergic and conflicting services [23].

Recognizing that the district network operator (DNO) would have to compensate the district for using its flexibility to alleviate the local network constraint, revenue for a DNO service is included. This revenue is calculated by comparing district operational costs with and without the network constraint [23].

The district is made up of fifty well-insulated residential detached buildings, situated in the north of England. The district, as a whole, has an import/export limit of 85kVA. Base electricity load has a power factor of 0.92. Gas boilers and EHP are sized to heat the dwelling during design conditions ($T^{out}_{s,i}$ =-4°C and $T_{s,i,l} = 21$°C for all index values) while supplying the maximum possible DHW demand. Gas boiler efficiency is set to 75%, whilst EHP coefficient-of-performance (COP) is set according to the linear function for which COP=3.51 at 20°C and 1.97 at -4°C. For the TES $X^{max}_l = 55$°C and $X^{min}_l = 40$°C for all $l = 1$ to N_l. Temperature deficit and surplus penalties (ς^+_i, ς^-_i), assigned to deviations outside of the interval around the set temperature defined by $\delta^{high}_{i,l}$ and $\delta^{low}_{i,l}$, are set to £1000/°Ch [8]. BES round-trip efficiency is set to 90%. Energy and reserve prices are taken from the U.K. context. Deterministic energy price components are defined as in [35], whilst imbalance prices are defined using a scenario reduction approach as in [8]. Figure 1 shows energy and reserve prices for a typical winter weekday.

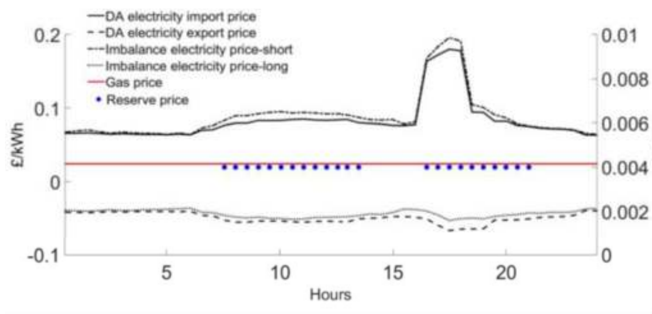

Fig. 1. Average energy and reserve prices for winter weekday representative day.

As in [8], the model is run for one day, separated into 48 time-steps, with each run having thirty scenarios, each with different imbalance price, environmental (temperature/insolation), occupancy, base electricity and DHW profiles. The thirty scenarios are set by combining ten imbalance price and three environmental scenarios, selected using the simultaneous backward reduction algorithm [36] which finds the most representative daily profiles of imbalance prices, solar insolation and outdoor temperature for each season, based on data from previous seasons. Occupancy, base electricity and DHW profiles are then taken from relevant profile libraries and assigned randomly [8]. Annual metrics are calculated by running the model for summer/shoulder (spring/autumn)/winter weekdays and weekends, and for a "peak" day (representing the 15 peak days of the year [35]), and weighting results accordingly (as in [8]). A graphical description of the overall process used to formulate the problem and run the case studies is given in Figure 2.

Run times vary within the range 5 minutes – 20 minutes, (3.6 GHz quad core processor, 32GB RAM). Hence the formulation is practical at the day-ahead stage.

A. EHP Integration

In the base test the number of EHPs in the district is increased incrementally until there is no feasible solution on the "peak" day. For the considered case study, it was found that 36 EHP could be accommodated. Then, for tests 1-6, EHP

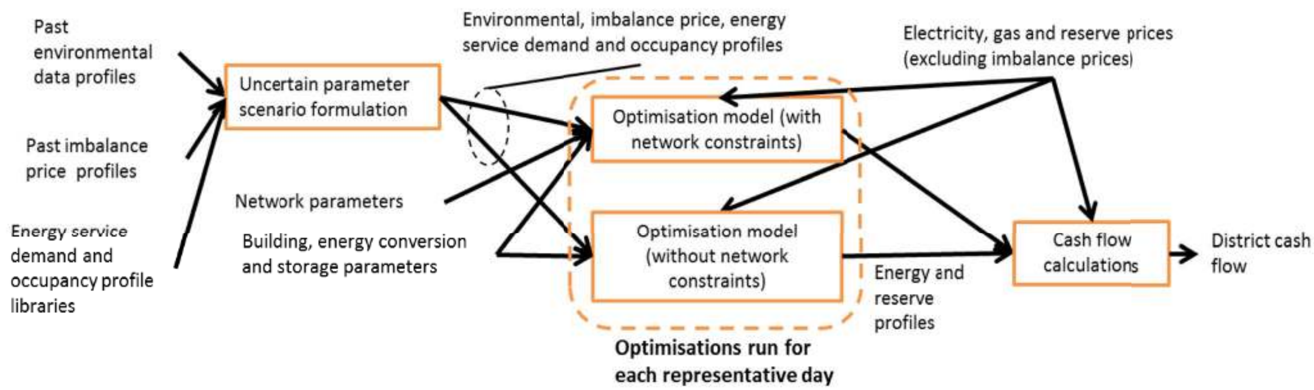

Fig. 2. Process for running and valuing the case studies.

TABLE II
SIZE OF FLEXIBLE RESOURCE, BY TEST, TEST 1-6

Test	Size of flexible resource, per building
1	230 litre TES
2	Auxiliary gas boiler, sized at 14% of peak load
3	5.5kWh/0.55kW[1] battery
4	4.5kWh/0.45kW battery, 0.675kVA inverter[2]
5	$\delta_{i,l}^{high}$=0.1
6	$\delta_{i,l}^{high}/\delta_{i,l}^{low}$=0.05

were placed in every building, and the flexibility was increased incrementally until the problem was feasible on the "peak" day. Table II shows the values for the relevant parameters for the type of flexibility considered in tests 1 to 6.

For tests 0-6, Figure 3 shows base load active and reactive power, EHP active power, and district maximum and average real power. Dependent on the test, series relating to the considered flexible resource are also shown. In all flexible tests, behavior can be seen to vary to maintain district import below the threshold, and to obtain benefits from energy arbitrage, given the "peak" day energy prices [35]. Here, import prices include energy prices, use-of-system fees and taxes, whilst export prices are comprised of only energy prices.

For test 0, Figure 3 demonstrates high EHP electricity import in the early hours of the morning. This may seem odd given the case has no explicit source of flexibility. However the result is enabled by constraints (5) and (6), which only constrain building temperature during times of active occupancy. This allows some flexibility to reduce energy costs and maintain net import below limits by enabling heat to be stored in the building fabric. As the buildings in this case are well-insulated, losses are low, and such storage is economic. Note that gas consumption, from use of the 14 gas boilers in the district, peaks later. This is due to the lack of net import constraints, and the flat gas price (see Figure 1), which means there is no motivation to store heat in the building fabric, to shift gas boiler gas consumption. Results for test 1 show an even greater shift of EHP operation to the low price, early morning periods. Heat is first directed to the TES (the more efficient heat store), and then to the building, again subject to constraints (5) and (6). TES heat is discharged over the morning and early evening peak electricity price period. Another result of the available flexibility in test 1, which can be seen in tests 2-6 also, is the greater total district electricity consumption, as the flexible resources enable more import.

For test 2, EHP electricity consumption again shifts to the early morning, but the lack of storage means that when base electricity load increases around 6am, it must decrease. Gas boiler operation occurs around 8am, at the local high price period, as this is the most cost-effective time for it to operate, to counter the morning peak (which is fluid to some extent, as building heat storage during non-occupancy allows it to be shifted, within limits determined by active occupancy and building thermal losses). Later gas boiler operation is economically rational, given high electricity prices, and necessary, to supply evening peak heat demand.

In test 3, BES allow the district to take advantage to the early morning low price period by shifting electricity import to those periods. Limited district import capacity means that the full capacity of the BES cannot be utilized. Some BES energy is discharged in the morning, to maintain district consumption below limits, but most is retained for the evening peak, which is also more economic given higher electricity prices in the evening. For test 4, results are similar to test 3, although there is notably greater use of the BES capacity (recall that BES capacity is smaller in test 4, compared to test 3). In this test, the evening peak in heat demand is accommodated through using the BES inverter to absorb the base load reactive power, at peak times.

In tests 5 and 6, flexibility enabled by the high/low building flexibility parameters ($\delta_{i,l}^{high}/\delta_{i,l}^{low}$) is demonstrated by the 'Average T surplus' and 'Average T deficit' series, which show the average deviation, during active occupancy, of the building temperature from the set temperature. In test 5, it can be seen that there is not a significant temperature surplus in the early hours of the morning, as low active occupancy in this period allows heat to be stored in the building fabric without raising the temperature for buildings with active occupancy. There is then a rise in the temperature surplus later in the morning, before a period of relatively high electricity price, during which heat stored in the building fabric is 'run down'.

[1]Battery power/energy ratio set at 10%.

[2]Battery inverter size set at 150% battery power rating.

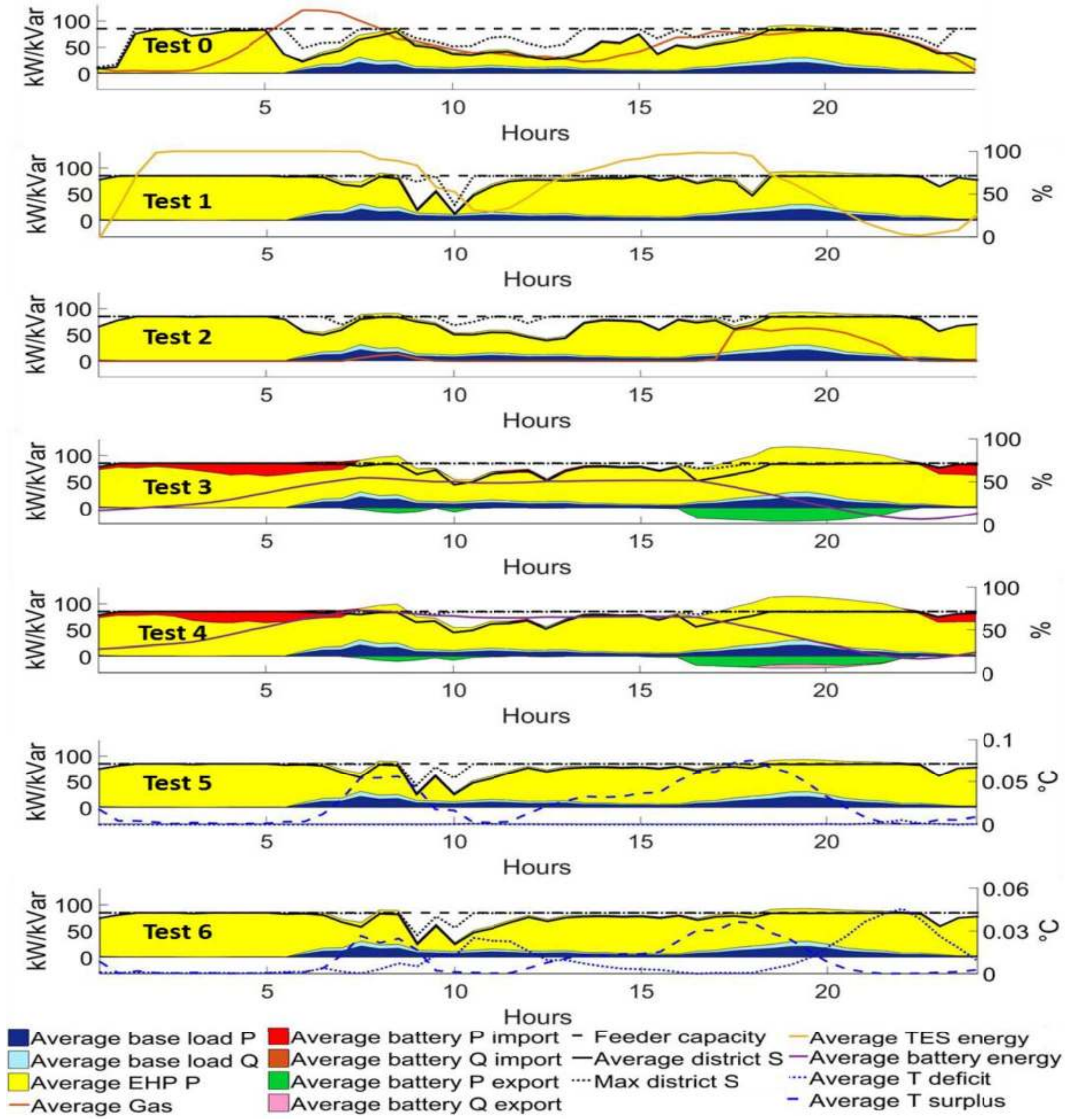

Fig. 3. Average baseload profiles, battery profiles, EHP power, gas consumption, storage states, and average and maximum district apparent power and feeder capacity, for tests 0-6 on a "peak day" representative day.

There is then another peak in temperature surplus later in the day, as heat is stored in the building fabric to reduce EHP operation during the very high price period, and to ensure electricity import is maintained below limits. In test 6, the building behavior is similar, but with variation in temperature split between the surplus and deficit variables.

Whilst all storage options enable the integration of an EHP for each house, it is notable that tests 5 and 6 illustrate that integration is enabled by very small deviations in the building temperature. These deviations may be so small as to be undetectable to building occupants. Thus, allowing the building temperature to vary slightly at peak times may be a low cost solution to enable EHPs (or other large loads) without additional infrastructure.

B. Reserve Provision

For tests 7-12 the reserve product is based on the U.K. short term operating reserve product, adopting the same windows (approximately 0700-1300, 1600-2030, though varying slightly by season), with reserve calls limited to 30 minutes. There are assumed to be 100 calls for the reserve product per year, resulting in a value of 0.014 for P^{dcall}. In the tests presented in Figure 4 an enhanced reserve price (x10) is used to better demonstrate model behavior, as the original price did not motivate significant behavior change.

In Figure 4 the series related to tests 7-12 are suffixed with 'w/r' (with reserve). Equivalent tests without reserve (see Table I) are suffixed with 'n/r' (no reserve). Comparing test 7 with test 1, Figure 4 shows a change in EHP operation, in

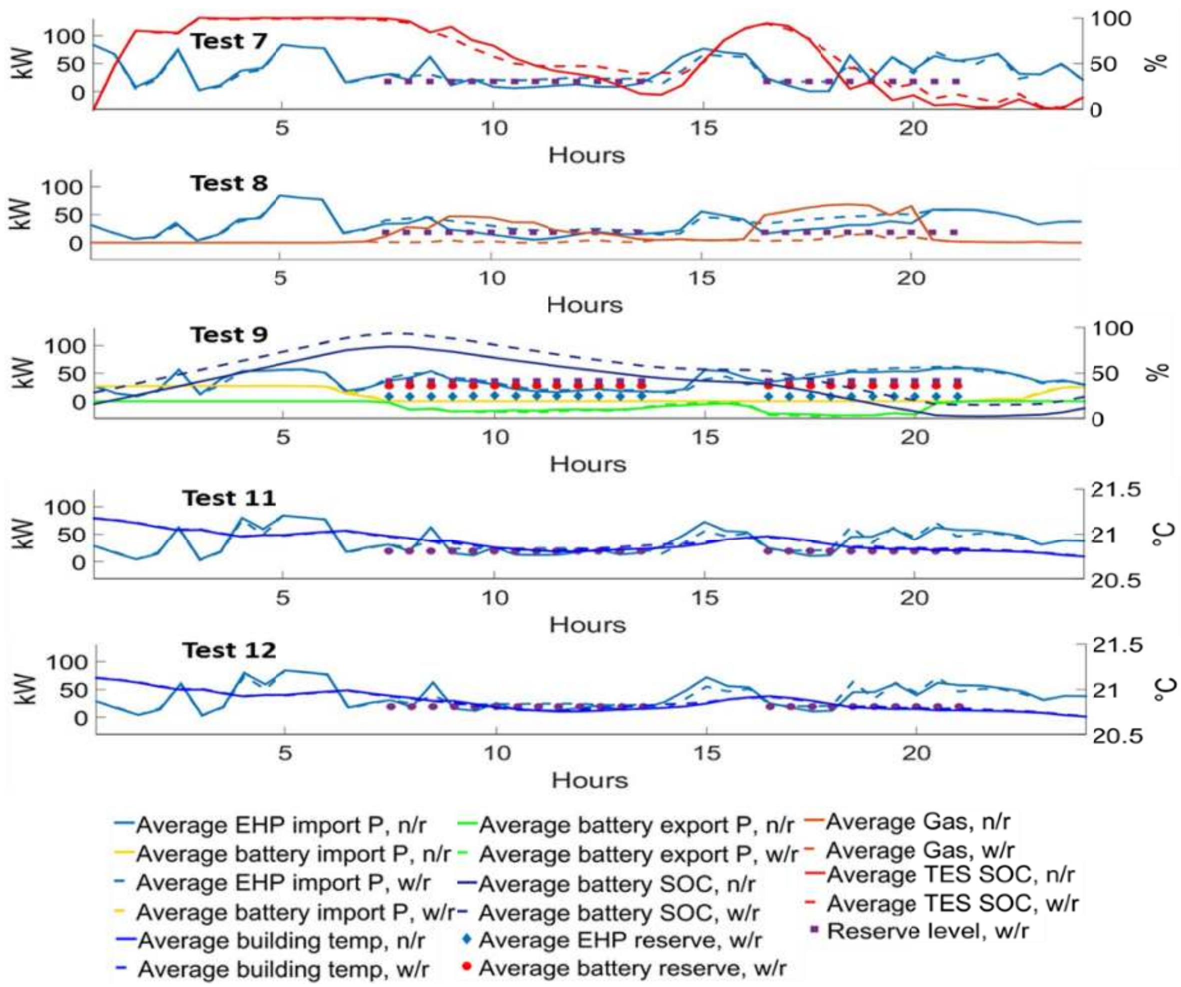

Fig. 4. Average EHP power, battery import/export, storage states and battery, EHP and overall reserve commitment, for tests 7-9, 11-12, for a winter weekday representative day (n/r=no reserve, w/r=with reserve).

order that minimum EHP power consumption over the reserve period is increased, in order to provide reserve. In particular, a local peak around 8am is reduced, with increased operation over the periods 10am-1pm and 5pm-6pm to compensate. An increase in minimum TES state-of-charge (SOC) during reserve hours can also be observed, as heat is retained to ensure the solution is robust to any reserve call. Note that the minimum point of the average EHP consumption series may be greater than the reserve provided, as the amount of reserve committed must be available across all scenarios.

Considering test 8, a reduction in gas boiler operation, compared to test 2, can be observed in Figure 4. This is a result of the shift to EHP heat provision, to increase the minimum EHP power consumption during reserve periods, to increase the amount of reserve that can be provided.

Comparing test 9 and test 3, the operation of the flexible devices is quite similar, with only a slight increase in EHP power consumption during reserve periods. However, the model, in which initial and final battery SOC is not set, maintains a generally increased battery SOC in test 9. This is so that the battery can contribute more reserve. Given the similarity of the test 10 vs. test 4 comparison, to the test 9 vs. test 3 comparison (as, in season 5, the district import does not near capacity, so there is no reactive power compensation), this comparison in not shown in Figure 4.

Test 11 vs. test 5 shows, as with the test 6/1 comparison, reduction of a local EHP consumption peak around 8am, which enables increased consumption (to increase the reserve available) between approximately 10am-1pm. This, and an increase in operation in the 5pm-6pm period, is enabled by exploiting building thermal storage. Initially the temperature (compared to test 5) is reduced, before being increased and then increasing in the middle of the day, as EHP operation is increased, before being reduced once more, to enable the later increase in heat production. Note that, even though test 11 featured a [$T_{i,l}^{set}$, $T_{i,l}^{set}$+0.1°C] feasible zone, temperature may be decreased during non-occupancy, allowing temperature in test 11 to deviate down as well as up compared to test 5.

In the test 12 vs. test 6 comparison, the trends as the same as identified in the test 11 vs. test 6 comparison, though with temperatures generally reduced (due to the reduced limit of the temperature feasible zone), and with the EHP consumption also slightly reduced.

These results indicate the power of flexible devices to offer reserve without compromising (outside of set boundaries) user comfort and without violating network constraints. These results may have relatively small revenue effects

TABLE III
CHANGE IN ETD, COMPARED TO TEST 0, SELECTED CASES

Test	Change in ETD (°Ch/year)
5	7463
6	6170
11	7524
12	6156

(see Section III-C), but indicate the viability of multi-service provision, which may be more valuable for differently parameterized districts, or for more lucrative reserve products (such as new 'fast' frequency response services designed to provide 'synthetic inertia' [37]).

C. Cash Flow Results

Collating results from the various seasons, changes in annual district revenue, for each test compared to the base test (0) is presented in Figure 5. Figure 5 shows that the greatest increases in district revenue (equivalently, costs savings), occur for tests 1, 5-7 and 11-12. This occurs for two reasons. Firstly, these tests rely on the EHP for heat provision, which is generally produces heat cheaper than the gas boiler, without use of the battery (operation of which results in losses, due to the 90% round-trip efficiency). Secondly, compared to the battery cases (3-4 and 9-10) there is more revenue from the DNO service in these tests. This is because, without the network limit, the EHP COP motivates shift of heat production towards times of higher outdoor temperature, including evening, high demand, periods. Imposition of the limit thus results in significant change in behavior, as demand is shifted away from these periods, particularly towards to the very high price period (1700-1800), producing significant additional cost.

Considering the reserve tests (7-12), the BES tests (9-10) produce the most significant reserve revenue. This is because the amount of energy stored in the BES over the day can be generally increased (as shown in Figure 4, albeit for the enhanced reserve price) to provide the energy to enable robust reserve commitments to be made. In these tests there is limited conflict with energy arbitrage as the charge/discharge limits of the battery mean that the BES cannot vary over its full capacity range, within the low/high energy price cycle (see Figure 4).

Overall, the tests with TES and building temperature flexibility (1, 5-7 and 11-12) appear to produce the greatest benefit. However, it should be recalled that tests 5-6 and 11-12 rely on varying the building temperature during times of active occupancy, and therefore incurs costs not shown in Figure 5, relating to expected thermal discomfort (ETD). For the relevant tests the changes in ETD, for all houses in the district, is shown in Table III.

As previously discussed in [8] these costs are borne by the end-user, who should be compensated for their loss of comfort. In reality, given the small deviations involved, which are likely to be undetectable, this may not be necessary. These costs could be significantly reduced if a price of thermal discomfort could be determined and building thermal inertia could be exploited through incorporating the ETD cost into the objective function.

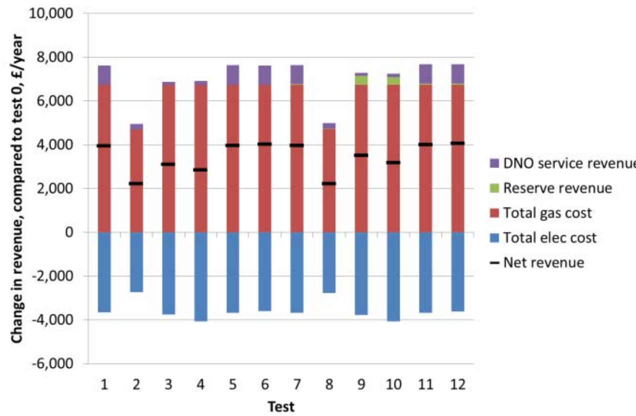

Fig. 5. Change in district revenue, by test, compared to test 0.

IV. CONCLUSION

This paper has presented a comprehensive two-stage stochastic smart district optimization model for multi-energy communities. The model allows for various flexible conversion and storage devices (i.e., CHP, EHP, EB, TES and BES), all types of district flexibility (*multi-energy storage* – namely, electrical and thermal, *substitution*, *curtailment* and *power factor manipulation*), both energy and reserve markets, and consideration of local constraints. Specific constraints ensure reserve provision from electro-thermal resources is robust against any reserve call with respect to thermal comfort. This comprehensive, multi-energy formulation offers a significant contribution above existing literature, and is a powerful tool to compare, value and maximize flexibility in communities.

Case studies on a synthetic district operating near its import limit have demonstrated practical applications of the model. Specifically, the model was used to show how the various types of flexibility available in a smart district can enable integration of EHP. Similarly, integration of any other significant new loads/electricity generators (e.g., electric vehicles, solar photovoltaic) could be modelled. Subsequently, the possibility to use the implemented flexibility to provide system operating reserve, without the risk of degrading building occupant thermal comfort, was demonstrated. The change in operational revenue for each case relative to a base case was shown. A key result enabled by the presented formulation and demonstrated by the case study is the ability of various types of flexibility to ameliorate network constraints caused by adoption of electric heating (or other large loads). Of particular note is the degree by which EHP integration can be aided by allowing the temperature of buildings to vary by a small degree, though the effect on thermal comfort experienced by occupants requires further investigation. Demonstration of the ability of the flexible resources to provide multiple services is another key result. The profitability of this ability is limited in this case, but may be larger for different districts, and if considering different services, e.g., new 'fast' frequency response services designed to provide 'synthetic inertia'. Overall, the ability of the formulation to compare the various types of flexibility within one framework presents a clear advantage which aids a technology and energy vector agnostic assessment of district flexibility.

Future work will consider incorporating assessment of battery degradation into the optimization and revenue evaluation, considering the varying effect different business cases have on battery utilization and hence degradation. The ability of other power electronic interfaced technologies, such as the EHP, to offer reactive power compensation, which could also aid EHP integration, will also be investigated.

REFERENCES

[1] G. Strbac, D. Pudjianto, P. Djapic, and S. Gammons, "Understanding the balancing challenge," Imperial College London, London, U.K., Tech. Rep., Aug. 2012.

[2] S. Althaher, P. Mancarella, and J. Mutale, "Automated demand response from home energy management system under dynamic pricing and power and comfort constraints," *IEEE Trans. Smart Grid*, vol. 6, no. 4, pp. 1874–1883, Jul. 2015.

[3] N. Good, K. A. Ellis, and P. Mancarella, "Review and classification of barriers and enablers of demand response in the smart grid," *Renew. Sustain. Energy Rev.*, vol. 72, pp. 57–72, May 2017.

[4] E. A. Martínez-Ceseña, N. Good, and P. Mancarella, "Electrical network capacity support from demand side response: Techno-economic assessment of potential business cases for small commercial and residential end-users," *Energy Policy*, vol. 82, pp. 222–232, Jul. 2015.

[5] K. McKenna and A. Keane, "Residential load modeling of price-based demand response for network impact studies," *IEEE Trans. Smart Grid*, vol. 7, no. 5, pp. 2285–2294, Sep. 2016.

[6] B. P. Koirala, E. Koliou, J. Friege, R. A. Hakvoort, and P. M. Herder, "Energetic communities for community energy: A review of key issues and trends shaping integrated community energy systems," *Renew. Sustain. Energy Rev.*, vol. 56, pp. 722–744, Apr. 2016.

[7] N. Good, E. A. M. Ceseña, and P. Mancarella, "Ten questions concerning smart districts," *Build. Environ.*, vol. 118, pp. 362–376, Jun. 2017.

[8] N. Good, E. Karangelos, A. Navarro-Espinosa, and P. Mancarella, "Optimization under uncertainty of thermal storage-based flexible demand response with quantification of residential users' discomfort," *IEEE Trans. Smart Grid*, vol. 6, no. 5, pp. 2333–2342, Sep. 2015.

[9] M. Geidl and G. Andersson, "Optimal power flow of multiple energy carriers," *IEEE Trans. Power Syst.*, vol. 22, no. 1, pp. 145–155, Feb. 2007.

[10] A. Martinez-Mares and C. R. Fuerte-Esquivel, "A robust optimization approach for the interdependency analysis of integrated energy systems considering wind power uncertainty," *IEEE Trans. Power Syst.*, vol. 28, no. 4, pp. 3964–3976, Nov. 2013.

[11] N. Neyestani, M. Yazdani-Damavandi, M. Shafie-khah, G. Chicco, and J. P. S. Catalao, "Stochastic modeling of multienergy carriers dependencies in smart local networks with distributed energy resources," *IEEE Trans. Smart Grid*, vol. 6, no. 4, pp. 1748–1762, Jul. 2015.

[12] P. Mancarella, "MES (multi-energy systems): An overview of concepts and evaluation models," *Energy*, vol. 65, pp. 1–17, Feb. 2014.

[13] R. Moreno, R. Moreira, and G. Strbac, "A MILP model for optimising multi-service portfolios of distributed energy storage," *Appl. Energy*, vol. 137, pp. 554–566, Jan. 2015.

[14] O. Mégel, J. L. Mathieu, and G. Andersson, "Scheduling distributed energy storage units to provide multiple services under forecast error," *Elect. Power Energy Syst.*, vol. 72, pp. 48–57, Nov. 2015.

[15] X. He, E. Delarue, W. D'Haeseleer, and J.-M. Glachant, "A novel business model for aggregating the values of electricity storage," *Energy Policy*, vol. 39, no. 3, pp. 1575–1585, 2011.

[16] W. B. Powell and S. Meisel, "Tutorial on stochastic optimization in energy—Part I: Modeling and policies," *IEEE Trans. Power Syst.*, vol. 31, no. 2, pp. 1459–1467, Mar. 2016.

[17] X. Xi, R. Sioshansi, and V. Marano, "A stochastic dynamic programming model for co-optimization of distributed energy storage," *Energy Syst.*, vol. 5, no. 3, pp. 475–505, 2014.

[18] X. Xi and R. Sioshansi, "A dynamic programming model of energy storage and transformer deployments to relieve distribution constraints," *Comput. Manag. Sci.*, vol. 13, no. 1, pp. 119–146, 2016.

[19] B. Cheng and W. Powell, "Co-optimizing battery storage for the frequency regulation and energy arbitrage using multi-scale dynamic programming," *IEEE Trans. Smart Grid*, to be published, doi: 10.1109/TSG.2016.2605141.

[20] F. Teng and G. Strbac, "Business cases for energy storage with multiple service provision," *J. Modern Power Syst. Clean Energy*, vol. 4, no. 4, pp. 615–625, 2016.

[21] J. Jin and Y. Xu, "Optimal storage operation under demand charge," *IEEE Trans. Power Syst.*, vol. 32, no. 1, pp. 795–808, Jan. 2017.

[22] C. Goebel and H.-A. Jacobsen, "Bringing distributed energy storage to market," *IEEE Trans. Power Syst.*, vol. 31, no. 1, pp. 173–186, Jan. 2016.

[23] R. Moreira, R. Moreno, and G. Strbac, "Synergies and conflicts among energy storage services," in *Proc. EnergyCon*, Leuven, Belgium, 2016, pp. 1–6.

[24] P. Mancarella and G. Chicco, "Real-time demand response from energy shifting in distributed multi-generation," *IEEE Trans. Smart Grid*, vol. 4, no. 4, pp. 1928–1938, Dec. 2013.

[25] J. Hong, N. J. Kelly, I. Richardson, and M. Thomson, "Assessing heat pumps as flexible load," *Proc. Inst. Mech. Eng. A J. Power Energy*, vol. 227, no. 1, pp. 30–42, Sep. 2012.

[26] D. Patteeuw *et al.*, "Integrated modeling of active demand response with electric heating systems coupled to thermal energy storage systems," *Appl. Energy*, vol. 151, pp. 306–319, Aug. 2015.

[27] O. Kilkki, A. Alahäivälä, and I. Seilonen, "Optimized control of price-based demand response with electric storage space heating," *IEEE Trans. Ind. Informat.*, vol. 11, no. 1, pp. 281–288, Feb. 2015.

[28] D. Schüwer, C. Krüger, F. Merten, and A. Nebel, "The potential of grid-orientated distributed cogeneration on the minutes reserve market and how changing the operating mode impacts on CO2 emissions," *Energy*, vol. 110, pp. 23–33, Sep. 2016.

[29] T. Muche, C. Höge, O. Renner, and R. Pohl, "Profitability of participation in control reserve market for biomass-fueled combined heat and power plants," *Renew. Energy*, vol. 90, pp. 62–76, May 2016.

[30] J. Haakana, V. Tikka, J. Lassila, and J. Partanen, "Methodology to analyze combined heat and power plant operation considering electricity reserve market opportunities," *Energy*, vol. 127, pp. 408–418, May 2017.

[31] S. H. Tindemans, V. Trovato, and G. Strbac, "Decentralized control of thermostatic loads for flexible demand response," *IEEE Trans. Control Syst. Technol.*, vol. 23, no. 5, pp. 1685–1700, Sep. 2015.

[32] V. Trovato, S. H. Tindemans, and G. Strbac, "Leaky storage model for optimal multi-service allocation of thermostatic loads," *IET Gener. Transm. Distrib.*, vol. 10, no. 3, pp. 585–593, Feb. 2016.

[33] D. Patteeuw *et al.*, "Integrated modeling of active demand response with electric heating systems," *Appl. Energy*, vol. 151, pp. 306–319, Aug. 2014.

[34] N. Good and P. Mancarella, "Modelling and assessment of business cases for smart multi-energy districts," in *Proc. PSCC*, Genoa, Italy, 2016, pp. 1–7.

[35] N. Good, E. A. Martínez-Ceseña, L. Zhang, and P. Mancarella, "Techno-economic and business case assessment of low carbon technologies in distributed multi-energy systems," *Appl. Energy*, vol. 167, pp. 158–172, Apr. 2016.

[36] H. Heitsch and W. Römisch, "Scenario reduction algorithms in stochastic programming," *Comput. Optim. Appl.*, vol. 24, nos. 2–3, pp. 187–206, 2003.

[37] *Enhanced Frequency Response Market Information Report*, Nat. Grid, Warwick, U.K., pp. 1–3, 2016.

Nicholas Good (S'11–M'15) received the Ph.D. degree in electrical engineering from the University of Manchester, where he is currently a Research Associate with Smart Urban Energy Systems. His research interests include optimization of flexible multienergy systems under uncertainty, associated business case development, and related socio-technical aspects.

Pierluigi Mancarella (M'08–SM'14) received the M.Sc. and Ph.D. degrees in electrical energy systems from the Politecnico di Torino, Turin, Italy, in 2002 and 2006, respectively. He is currently a Chair Professor of electrical power systems with the University of Melbourne, Australia, and a Professor of Smart Energy Systems, University of Manchester, U.K. His research interests include multienergy systems, power system integration of low carbon technologies, network planning under uncertainty, and risk and resilience of smart grids. He is an Editor of the IEEE TRANSACTIONS ON SMART GRID, an Associate Editor of the IEEE Systems Journal, and an IEEE PES Distinguished Lecturer.